J|A|C|S
ARTICLES
Published on Web 06/11/2002

Combined Solid State NMR and X-ray Diffraction Investigation of the Local Structure of the Five-Coordinate Silicon in Fluoride-Containing As-Synthesized STF Zeolite

Colin A. Fyfe,*,† Darren H. Brouwer,† Andrew R. Lewis,† Luis A. Villaescusa,‡ and Russell E. Morris*,‡

Contribution from the Department of Chemistry, University of British Columbia, 2036 Main Mall, Vancouver, BC, V6T 1Z1, Canada, and School of Chemistry, University of St. Andrews, Purdie Building, St. Andrews KY16 9ST, United Kingdom

Received November 16, 2001. Revised Manuscript Received March 18, 2002

Abstract: The local structure of the $[SiO_{4/2}F]^-$ unit in fluoride-containing as-synthesized STF zeolite has been experimentally determined by a combination of solid-state NMR and microcrystal X-ray diffraction to be very close to trigonal bipyramidal. Because the fluoride ions are disordered over two sites, the resulting local structure of the $[SiO_{4/2}F]^-$ unit from a conventional XRD refinement is an average between tetrahedral $SiO_{4/2}$ and five-coordinate $[SiO_{4/2}F]^-$, giving an apparent F−Si distance longer than expected. The correct F−Si distance was determined by slow spinning MAS and fast spinning $^{19}F/^{29}Si$ CP and REDOR solid-state NMR experiments and found to be between 1.72 and 1.79 Å. In light of this, the X-ray structure was re-refined, including the disorder at Si3. The resulting local structure of the $[SiO_{4/2}F]^-$ unit was very close to trigonal bipyramidal with a F−Si distance of 1.744 (6) Å, in agreement with the NMR results and the prediction of Density Functional Theory calculations. In addition, further evidence for the existence of a covalent F−Si bond is provided by a $^{19}F\rightarrow^{29}Si$ refocused INEPT experiment. The resonance for the five-coordinate species at −147.5 ppm in the ^{29}Si spectrum is a doublet due to the $^{19}F/^{29}Si$ *J*-coupling of 165 Hz. The peaks in this doublet have remarkably different effective chemical shift anisotropies due to the interplay of the CSA, dipolar coupling, and *J*-coupling tensors. The distortions from tetrahedral geometry of the neighboring silicon atoms to the five-coordinate Si3 atom are manifested in increased δ_{aniso} values. This information, along with F−Si distances measured by $^{19}F\rightarrow^{29}Si$ CP experiments, makes it possible to assign half of the ^{29}Si resonances to unique tetrahedral sites. As well as determining the local geometry of the $[SiO_{4/2}F]^-$ unit, the work presented here demonstrates the complementarity of the solid-state NMR and X-ray diffraction techniques and the advantages of using them together.

Introduction

The preparation of zeolites and related microporous materials from fluoride-containing media[1−7] has led to the synthesis of new low framework density zeolite phases,[6] pure silica zeolites with very few framework defects,[8,9] large zeolite crystals,[10] unique nonlinear optical materials,[11] and many new $AlPO_4$ and $GaPO_4$ structures.[4,7,12] Consequently, there has been considerable interest in understanding how the fluoride ions are involved in controlling the structure and properties of these materials.

Two main functions of the fluoride ions have been proposed: acting as a mineralizing agent by which the solubility of the silicate ions at neutral pH is improved and as a catalyst of the condensation reaction involved in the formation of Si−O−Si bonds.[13] Solid-state NMR spectroscopy[14−16] and X-ray diffraction (XRD) studies[11,17−20] have revealed that the fluoride ions are often directly connected to the frameworks of as-synthesized zeolite structures as five-coordinate $[SiO_{4/2}F]^-$ units.

* Corresponding author. E-mail: fyfe@chem.ubc.ca.
† University of British Columbia.
‡ University of St. Andrews.

(1) Flanigen, E. M.; Patton, R. L. U.S. Patent No. 4073865, 1978.
(2) Guth, J. L.; Kessler, H.; Wey, R. In *New Developments in Zeolite Science and Technology, Proceedings of the 7th International Zeolite Conference*; Murakami, Y., Iijima, A., Ward, J. W., Eds.; Elsevier: Amsterdam, The Netherlands, 1986; p 121.
(3) Guth, J. L.; Kessler, H.; Higel, J. M.; Lamblin, J. M.; Patarin, J.; Seive, A.; Chézeau, J. M.; Wey, R. *Am. Chem. Soc. Symp. Ser.* **1989**, *389*, 176.
(4) Guth, J. L.; Kessler, H.; Caullet, P.; Hazm, J.; Merrouche, A.; Patarin, J. In *Proceedings from the 9th International Zeolite Conference*; von Ballmoos, R., Higgins, J. B., Treacy, M. M. J., Eds.; Butterworth-Heinemann: Stoneham, MA, 1993; Vol. I, p 215.
(5) Kessler, H.; Patarin, J.; Schott-Darie, C. *Stud. Surf. Sci. Catal.* **1994**, *85*, 75.
(6) Camblor, M. A.; Villaescusa, L. A.; Díaz-Cabañas, M. J. *Top. Catal.* **1999**, *9*, 59.
(7) Wragg, D. S.; Slawin, A. M. Z.; Morris, R. E. *J. Mater. Chem.* **2001**, *11*, 1850.
(8) Chézeau, J. M.; Delmotte, L.; Guth, J. L.; Soulard, M. *Zeolites* **1989**, *9*, 78.
(9) Chézeau, J. M.; Delmotte, L.; Guth, J. L.; Gabelica, Z. *Zeolites* **1991**, *11*, 598.
(10) Kuperman, A.; S., N.; Oliver, S.; Ozin, G. A.; Garces, J. M.; Olken, M. M. *Nature* **1993**, *365*, 239.
(11) Bull, I.; Villaescusa, L. A.; Teat, S. J.; Camblor, M. A.; Wright, P. A.; Lightfoot, P.; Morris, R. E. *J. Am. Chem. Soc.* **2000**, *122*, 7128.
(12) Matijasic, A. M.; Paillaud, J. L.; Patarin, J. *J. Mater. Chem.* **2000**, *10*, 1345.
(13) Barrett, P. A.; Camblor, M. A.; Corma, A.; Jones, R. H.; Villaescusa, L. A. *J. Phys. Chem. B* **1998**, *102*, 4147.
(14) Koller, H.; Wölker, A.; Eckert, H.; Panz, C.; Behrens, P. *Angew. Chem., Int. Ed. Engl.* **1997**, *36*, 2823.
(15) Koller, H.; Wölker, A.; Villaescusa, L. A.; Díaz-Cabañas, M. J.; Valencia, S.; Camblor, M. A. *J. Am. Chem. Soc.* **1999**, *121*, 3368.
(16) Fyfe, C. A.; Brouwer, D. H.; Lewis, A. R.; Chézeau, J. M. *J. Am. Chem. Soc.* **2001**, *123*, 6882.

10.1021/ja012558s CCC: $22.00 **© 2002 American Chemical Society**

Therefore, other functions for the fluoride ions have been postulated. For pure silica zeolites, the negative fluoride ions balance the charge of the positive structure directing agents (SDAs), a condition that is met by connectivity defect sites or the presence of aluminum in zeolites synthesized under other conditions. In the case of one pure silica as-synthesized IFR zeolite,[11,20] the fluoride ions not only balance the charge of the SDA cations, but also align and order the noncentrosymmetric SDA cations via electrostatic interactions to give a material with nonlinear optical properties. Electrostatic interactions between the fluoride ions and SDA cations may also be responsible for registering intermediate layers as they come together to form three-dimensional zeolite frameworks.[16] The crystal structures of pure silica zeolites prepared via the fluoride route reveal that the fluoride ions are located in small cages of the framework[11,16−21] and are often connected to silicon atoms that are part of four-membered rings.[11,16,18−20] Therefore, the fluoride ions may also have structure directing functions by energetically stabilizing small cages and/or four-membered rings.

It is clear that structural information on these fluoride-containing zeolites will be invaluable toward understanding how fluoride ions are involved in controlling their structures and properties. However, despite the importance of fluoride ions in this synthesis method, there are limited structural data concerning the location of fluoride ions in pure silica zeolite frameworks as conventional single-crystal XRD is limited in its application to zeolites due to their microcrystalline nature and to problems arising from twinning. Solid-state NMR[16] and single-crystal XRD of very small crystals with synchrotron radiation[11,19,20] have proven to be valuable methods to obtain structural information on fluoride-containing zeolites.

Koller and co-workers[14,15] have shown that the presence of five-coordinate $[SiO_{4/2}F]^-$ units in as-synthesized pure silica zeolites can be detected by solid-state ^{29}Si NMR spectroscopy, as these five-coordinate sites give resonances which, in the absence of fluoride ion motion, are shifted to about −145 to −150 ppm. If the fluoride ions are mobile between different silicon tetrahedra, a broad averaged resonance at about −125 ppm results. For those zeolites in which fluoride ion motion was absent, the five-coordinate peak was split into a *J*-coupling doublet with unequal intensities. Although not discussed in detail, Koller and co-workers identified the source of these unequal intensities as complications involving the interplay of the *J*-coupling, dipolar coupling, and chemical shift anisotropy tensors.[22−25] In fact, as we show in this paper, an analysis of the spinning sideband manifold of the peaks for the five-coordinate species can yield the $^{19}F/^{29}Si$ dipolar coupling and the F−Si internuclear distance.

In a previous publication,[16] we determined the average location of the fluoride ion undergoing dynamic disorder in [F,-TPA]-MFI by solid-state NMR techniques alone. This location was determined by measuring the F−Si internuclear distances by CP, REDOR, and TEDOR experiments to several different silicon T-sites which were assigned by the INADEQUATE experiment. The fluoride ion was found to be covalently bonded to Si9 in the $[4^15^26^2]$ cage of the MFI framework and exchanging between two "mirror-related" Si9 sites. Due to this dynamic disorder, the fluoride ion location and F−Si distances determined reflect the average local structure of the $[SiO_{4/2}F]^-$ unit, but it was clearly recognized that they did not provide the exact fluoride location or an accurate F−Si distance for the $[SiO_{4/2}F]^-$ unit.

Similarly, the local structures of the $[SiO_{4/2}F]^-$ units reported in XRD crystal structures may also not reflect the true local structure, but rather some average between $[SiO_{4/2}F]^-$ and $SiO_{4/2}$ units due to incomplete occupancy of the fluoride ions in the form of static[17,18,20] or dynamic[11,16,19,26] disorder. One consequence of this averaging is that the reported F−Si distances, between 1.84 and 1.99 Å, are longer than expected for a five-coordinate geometry. Attfield and co-workers recognized this problem and performed Density Functional Theory simulations on fluoride ions in SOD and FER frameworks.[27] They calculated the geometry of the $[SiO_{4/2}F]^-$ units and yielded predicted structures very close to trigonal bipyramidal with the Si−F distances (1.71 and 1.76 Å) much shorter than those obtained from previous XRD studies.

Since solid-state NMR probes local order, it should be possible to make experimental measurements on the F−Si internuclear distance in the $[SiO_{4/2}F]^-$ units which will not be susceptible to the averaging problems of incomplete occupancy and/or disorder which can effect XRD. Cross Polarization (CP)[28−33] and Rotational Echo Double Resonance (REDOR)[34,35] experiments which probe the heteronuclear dipolar coupling between nuclei have been demonstrated to be reliable in measuring distances between isolated $^{19}F/^{29}Si$ spin pairs in octadecasil[28,36,37] and [F,TPA]-MFI.[16] With information about the F−Si distance from these solid-state NMR experiments, the crystal structure can be reliably refined by including the disorder between $[SiO_{4/2}F]^-$ and $SiO_{4/2}$ at the T-site where the fluoride ions bond. Such a refinement is expected to come very close to describing the true geometry of the $[SiO_{4/2}F]^-$ unit.

As-synthesized zeolite with the STF framework[20,38,39] is a promising framework structure in which to study the detailed geometry of the $[SiO_{4/2}F]^-$ unit by both solid-state NMR and

(17) Attfield, M. P.; Weigel, S. J.; Taulelle, F.; Cheetham, A. K. *J. Mater. Chem.* **2000**, *10*, 2109.
(18) van de Goor, G.; Freyhardt, C. C.; Behrens, P. *Z. Anorg. Allg. Chem.* **1995**, *621*, 311.
(19) Camblor, M. A.; Díaz-Cabañas, M.-J.; Perez-Pariente, J.; Teat, S. J.; Clegg, W.; Shannon, I. J.; Lightfoot, P.; Wright, P. A.; Morris, R. E. *Angew. Chem., Int. Ed. Engl.* **1998**, *37*, 2122.
(20) Villaescusa, L. A.; Wheatley, P. S.; Bull, I.; Lightfoot, P.; Morris, R. E. *J. Am. Chem. Soc.* **2001**, *123*, 8797.
(21) Caullet, P.; Guth, J. L.; Hazm, J.; Lamblin, J. M.; Gies, H. *Eur. J. Solid State Inorg. Chem.* **1991**, *28*, 345.
(22) Cherryman, J. C.; Harris, R. K. *J. Magn. Reson.* **1997**, *128*, 21.
(23) Harris, R. K.; Packer, K.; Thayer, A. M. *J. Magn. Reson.* **1985**, *62*, 284.
(24) Harris, R. K.; Bai, H. *J. Magn. Reson.* **1992**, *96*, 24.
(25) Haubenreisser, U.; Sternberg, U. *Mol. Phys.* **1987**, *60*, 151.
(26) Aubert, E.; Porcher, F.; Souhassou, M.; Petricek, V.; Lecomte, C. *J. Phys. Chem. B* **2002**, *106*, 1110.
(27) Attfield, M. P.; Catlow, C. R. A.; Sokol, A. A. *Chem. Mater.* **2001**, *13*, 4708.
(28) Fyfe, C. A.; Lewis, A. R.; Chézeau, J. M. *Can. J. Chem.* **1999**, *77*, 1984.
(29) Hartmann, S. R.; Hahn, E. L. *Phys. Rev.* **1962**, *128*, 2042.
(30) Hediger, S. Improvement of Heteronuclear Polarization Transfer in Solid-State NMR, Ph.D. Dissertation, Eidgenössische Technische Hochschule, Zurich, Switzerland, 1997.
(31) Mehring, M. *Principles of High-Resolution NMR in Solids*, 2nd ed.; Springer-Verlag: Berlin, Germany, 1983.
(32) Pines, A.; Gibby, G.; Waugh, J. S. *J. Chem. Phys.* **1973**, *59*, 569.
(33) Stejskal, E. O.; Schaefer, J.; Waugh, J. S. *J. Magn. Reson.* **1977**, *28*, 105.
(34) Gullion, T.; Schaefer, J. *J. Magn. Reson.* **1989**, *81*, 196.
(35) Gullion, T.; Schaefer, J. *Adv. Magn. Reson.* **1989**, *13*, 57.
(36) Fyfe, C. A.; Lewis, A. R.; Chézeau, J. M.; Grondey, H. *J. Am. Chem. Soc.* **1997**, *119*, 12210.
(37) Bertani, P.; Raya, J.; Reinheimer, P.; Gougeon, R.; Delmotte, L.; Hirschinger, J. *Solid State Nucl. Magn. Reson.* **1999**, *13*, 219.
(38) Wagner, P.; Zones, S. I.; Davis, M. E.; Medrud, R. C. *Angew. Chem., Int. Ed. Engl.* **1999**, *38*, 1269.
(39) Villaescusa, L. A.; Barrett, P. A.; Camblor, M. A. *Chem. Commun.* **1998**, 2329.

X-ray diffraction. Crystals of [F,DMABO]-STF large enough for XRD investigations using a synchrotron source have been synthesized and the general framework structure has been established.[20] The fluoride ions exhibit static intercage disorder between fused $[4^15^26^2]$ cages. The local structure of the $[SiO_{4/2}F]^-$ unit was reported to be an average between five-coordinate and tetrahedral, although this disorder was not included in this refinement. Because the fluoride ions exhibit static disorder, rather than dynamic disorder, the ^{29}Si MAS NMR spectrum of this material has a relatively sharp resonance at about −148 ppm at room temperature due to the five-coordinate $[SiO_{4/2}F]^-$ unit, rather than a broad motionally averaged peak at about −125 ppm as observed in the room-temperature spectrum of [F,TPA]-MFI.[14−16] Consequently, measurements of the F−Si distance by solid-state NMR will be of the actual $[SiO_{4/2}F]^-$ unit rather than the motionally averaged distance over two or more sites.

The aim of the present work is to investigate experimentally, by a combination of solid-state NMR and X-ray diffraction, the detailed local geometry of the $[SiO_{4/2}F]^-$ units found in as-synthesized purely siliceous STF zeolites and to accurately determine the F−Si internuclear distance by ^{19}F/^{29}Si CP and REDOR experiments. In addition we also provide a detailed description of the observed behavior of the ^{19}F/^{29}Si *J*-coupling in these solid-state NMR experiments, including fast spinning and ^{19}F/^{29}Si INEPT experiments, and the results of a re-refinement of the XRD data.

Experimental Section

Samples. Two different cations were used as SDAs to synthesize the fluoride-containing STF pure silica zeolites, racemic *N,N*-dimethyl-6-azonium-1,3,3-trimethylbicyclo(3.2.1)octane (DMABO, **1**) and *N,N*-diethyl-*2,5-cis*-dimethylpiperidinium (DECDMP, **2**). The synthesis of

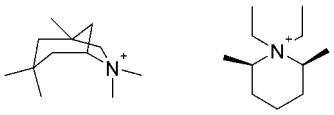

1 **2**

single crystals of [F,DMABO]-STF has been described previously.[20] The synthesis of [F,DECDMP]-STF was as follows: Tetraethyl orthosilicate (5.48 g) was hydrolyzed under stirring in 72.85 g of an aqueous solution of the hydroxide form of the organic cation (1.8×10^{-4} mol per gram of solution). The ethanol and almost all of the water are allowed to evaporate from the mixture. The resultant mixture is more a solid at this point, and after grinding it to a powder, HF (48%) was added and stirred by hand. In the case of DECDMP the solid was allowed to further evaporate water under vacuum to achieve the overall composition SiO_2:0.5DECDMPF:H_2O. The mixture was then heated in a Teflon-lined steel autoclave at 170 °C for 14 days under static conditions. The solid was washed with plenty of water and dried at 80 °C. A very crystalline white powder (1.34 g) was produced.

Solid-State NMR. Solid-state NMR experiments were performed on a Bruker AVANCE-400 spectrometer operating at frequencies of 400.13 MHz for ^{1}H, 376.434 MHz for ^{19}F, and 79.495 MHz for ^{29}Si. A Bruker 4 mm MAS probe, capable of spinning up to 15 kHz with the frequency controlled to ±5 Hz, was used for all experiments. The ^{19}F chemical shifts were referenced to $CFCl_3$ with octadecasil[21] as a secondary reference. The ^{29}Si chemical shifts were referenced to tetramethylsilane (TMS) with Q_8M_8 (the octamer $Si_8O_{12}[OSi(CH_3)_3]_8$) or octadecasil as an external secondary reference. Pulse lengths and cross polarization matching conditions were roughly determined on octadecasil and then accurately redetermined on the actual [F,-DECDMP]-STF sample. All spectra were collected at ambient temperature.

^{1}H→^{29}Si CP MAS spectra were collected with a contact time of 3 ms, a recycle time of 1.5 s (∼1.25T_1), and an acquisition time of about 50 ms during which a ^{1}H decoupling field of 80 kHz was applied. The 90° pulse length on the ^{1}H channel prior to the 80 kHz spin lock field was 3 μs. The matching conditions for ^{29}Si were set at the −1 spinning sideband matching condition using rf fields of 78 and 65 kHz for experiments at spinning rates of 1.9 and 15 kHz, respectively.

In all ^{19}F/^{29}Si experiments, the recycle time was 15 s (∼1.25T_1) and no decoupling was applied during the acquisition time. For ^{19}F→^{29}Si cross polarization, the 90° pulse length on the ^{19}F channel prior to the 55 kHz spin lock field was 4.6 μs. The matching conditions for ^{29}Si were set at the +1 spinning sideband condition using rf fields of 57 and 70 kHz for 1.9 and 15 kHz spin rates, respectively. The ^{19}F/^{29}Si CP-REDOR experiment was carried out at a spinning rate of 15 kHz with an initial ^{19}F→^{29}Si CP (0.4 ms contact time), using the conditions described above. The refocusing 180° pulse on ^{29}Si was 7.4 μs. The rotor-synchronized ^{19}F dephasing 180° pulses were 5.0 μs and followed *xy*-4 phase cycling (phase alternates between *x* and *y*). For the refocused INEPT experiment,[40,41] the 90° and 180° pulse lengths were 5.2 and 10.4 μs for both ^{19}F and ^{29}Si. The rotor-synchronized 1/(4*J*) echo time was set to 1.5 ms to maximize the transfer for a ^{19}F/^{29}Si *J*-coupling of 165 Hz. No decoupling was applied during the echo or acquisition times. Recycle times of ∼1.25T_1 were used in order to obtain optimal S/N in these experiments since the ^{19}F T_1 was long and many scans were required in the ^{1}H→^{29}Si CP MAS experiments. The use of recycle times less than 5T_1 is valid since there are single relaxation times for ^{19}F (a single site) and ^{1}H (a strongly coupled network).

Calculations. The deconvolution of spectra with Lorenztian peaks and the simulation and fitting of CP and REDOR curves were performed with progams written for Mathematica.[42] The simulation and fitting of the spinning sideband manifolds in the ^{19}F and ^{29}Si spectra were performed with the SIMPSON simulation program.[43]

Microcrystal X-ray Diffraction. The single crystals of [F,DMABO]-STF were too small (size 20 μm × 10 μm × 10 μm) for data collection on our in-house X-ray diffractometers, so microcrystal XRD was carried out at the CCLRC Daresbury Laboratory Synchrotron Radiation Source, Cheshire, UK, as previously described.[20] Refinements of the structural models were carried out with standard least-squares procedures, using the programs SHELXL-97[44] and WINGX.[45] Initially the average structural model of the framework was refined and the position of the $DMABO^+$ cation was found from successive difference Fourier maps to be disordered over two sites across the inversion center. SHELXL-97 "Same Distance" restraints were used to ensure that the refinement of the $DMABO^+$ cation was stable. The disorder due to the 50% occupancy of the fluoride site could not be resolved from difference Fourier maps and this was only accomplished after input of results from the NMR experiment (see below). The final agreement factor ($wR(F^2)$) converged to a relatively high value of 0.167, but the analysis of variance revealed no systematic errors in the refinement. The maximum and minimum final residual electron density peaks in the difference Fourier synthesis (1.70 and −1.71 eÅ^{-3}) were less than 1 Å from the closest atoms (O11 and C7, respectively), indicating that all atoms in the structure had been located successfully. The observed structure factor magnitudes for the weak reflections were slightly higher

(40) Fyfe, C. A.; Wong-Moon, K. C.; Huang, Y.; Grondey, H. *J. Am. Chem. Soc.* **1995**, *117*, 10397.
(41) Morris, G. A.; Freeman, R. *J. Am. Chem. Soc.* **1979**, *101*, 760.
(42) Wolfram, S. *Mathematica*, A System for Doing Mathematics by Computer v. 3.0; Wolfram Media: Champaign, IL, 1996.
(43) Bak, M.; Rasmussen, J. T.; Nielsen, N. C. *J. Magn. Reson.* **2000**, *147*, 296.
(44) Sheldrick, G. M. SHELX-97, Programs for Crystal Structure Analsysis v. 97−2; Institute fur Anorganische Chemie der Universitat, Tammanstrasse 4: D-3400 Gottingen, Germany, 1998.
(45) Farrugia, L. J. *J. Appl. Crystallogr.* **1999**, *32*, 837.

Table 1. Crystal Structure and Refinement Details for As-Made [F,DMABO]-STF Zeolite

sample title	[F,DMABO]-STF
chemical formula	$Si_{16}O_{32}.F.C_{12}H_{23}N$
unit cell	$a = 7.4573$ (2) Å
	$b = 18.0966$ (5) Å
	$c = 14.0233$ (4) Å
	$\beta = 99.254$ (1)^o
cell volume	1867.84 (9) Å^3 at $T = 150$ K
wavelength	0.6892 Å
Z	2
symmetry	monoclinic $P2_1/c$
no. of unique reflcns	5279
no. of obsd reflcns [$F^2 > 4\sigma(F^2)$]	4283
no. of parameters	339
$wR(F^2_{\text{obsd data}})$	0.167
$R(F_{\text{obsd data}})$	0.071
$S(F^2_{\text{all data}})$	1.064

than the calculated magnitudes. This is sometimes an indication of twinning of the crystal. However, a number of twinned models were tested and none proved to be an improvement when compared to the untwinned model. Included in twinned models tested was the expected twin for the STF framework based on a twin boundary made up of the very closely related SFF framework type.[38] Full structure determination parameters as well as final agreement factors are given in Table 1 and complete details of the refinement, atomic positions and bond distances can be found in the Supporting Information.

Results and Discussion

The basic framework topology of calcined siliceous STF zeolite was solved from powder XRD data by Camblor and co-workers,[39] confirmed independently by Wagner et al.,[38] and is shown in Figure 1a. It contains one-dimensional pores running along [001] with access through 10-membered-ring windows. The basic building unit consists of two fused [$4^15^26^2$] cages which link together to form the framework.

A single-crystal XRD study[20] of a fluoride-containing as-synthesized [F,DMABO]-STF confirmed the topology and found electron density due to disordered $DMABO^+$ cations in the large cavities (the cations were not modeled in the final refinement). The fluoride ions were disordered over two (equivalent) sites in the fused [$4^15^26^2$] cages, giving the average structure shown in Figure 1a. The F−Si distance was found to 1.87 Å. The local environment of the zeolite around one fluoride ion is shown in Figure 1b since only one cage of the fused pair is occupied by fluorine, with sixteen inequivalent sites as indicated. This model for the local environment was assumed in the investigation of the five-coordinate silicon.

Fast Spinning ^{29}Si Spectra. Unfortunately, the ^{29}Si MAS NMR spectrum of the [F,DMABO]-STF sample for which the single-crystal XRD data were collected was not of sufficient resolution to completely resolve individual ^{29}Si resonances. The broadening of the spectrum could be due to a number of reasons, including the presence of defect sites in the crystals, the disordering of the fluoride ions and SDA molecules, or the SDA molecules being a racemic mixture. However, highly resolved ^{29}Si NMR spectra were obtained for the [F,DECDMP]-STF sample and the solid-state NMR experiments were performed on this sample.

The fast spinning (15 kHz) ^{1}H→^{29}Si CP MAS spectrum of [F,DECDMP]-STF is shown in Figure 2a. The high resolution of the spectrum indicates that this is a very high quality sample

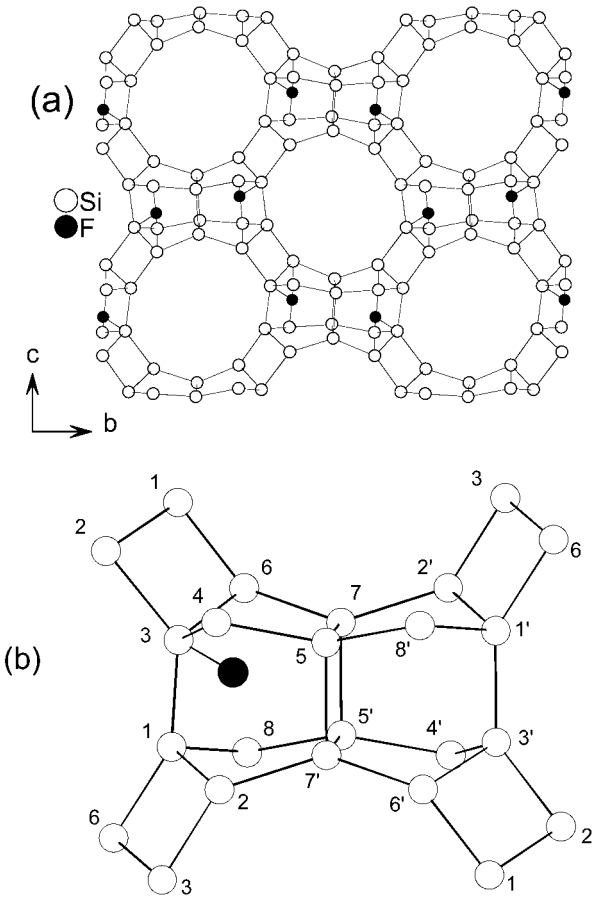

Figure 1. (a) Projection of the average structure of as-synthesized STF zeolite[20] on the (011) plane showing the disorder of the fluoride ions over two equivalent sites. Oxygen atoms are not shown and the occupancy for each fluorine site is 50%. (b) Numbering scheme for the silicon sites in the *local* environment about one fluorine since the fluoride ions occupy only one of the fused cage pairs.

with very few defects. The spectrum can be deconvoluted into twelve peaks and when the relative intensities are considered (Table 2), it becomes clear that it reflects 16 unique silicon sites in the structure. Although this ^{1}H→^{29}Si CP MAS spectrum cannot be assumed to be fully quantitative, it is expected to be reasonably close to being so since there are many protons well distributed throughout the structure and each silicon site is on the surface of the channels in which the SDA resides. Although the efficiency of the ^{1}H→^{29}Si CP MAS NMR experiment is limited by a short ^{1}H $T_{1\rho}$ relaxation time (3.4 ms), the short ^{1}H T_1 relaxation time (1.2 s) makes the CP experiment far more efficient than a ^{29}Si MAS NMR experiment (which would be fully quantitative) since the ^{29}Si T_1 relaxation time is very long (∼75 s).

At first sight, the observation of 16 peaks in the ^{29}Si MAS NMR spectrum of [F,DECDMP]-STF appears to be inconsistent with the eight crystallographically inequivalent sites in the XRD structure of [F,DMABO]-STF. However, it is important to remember that XRD probes the long-range order of the crystal, while solid-state NMR is sensitive to the local structure. The presence of 16 resonances in the ^{29}Si MAS NMR spectrum indicates that *on a local level*, the symmetry of the [F,DECDMP]-STF structure is indeed lower than that of the average crystal structure found for [F,DMABO]-STF which has disordered fluoride ions. The asymmetric unit of the crystal

Table 2. NMR Results and ^{29}Si Peak Assignments for [F,DECDMP]-STF

peak	δ_{iso} (ppm)[a]	rel intensity[a]	δ_{aniso} (ppm)[b]	F–Si dipolar coupling (kHz)[c]	F–Si distance from NMR (Å)[c]	assignment	F–Si distance from XRD[f] (Å)	predicted chemical shift[f,g] (ppm)
A	−147.6	0.93 (1)	74 ± 5	3.9 ± 0.4[d]	1.79 ± 0.06[(d)]	Si3	1.744 (7)	
				4.4 ± 0.4[e]	1.72 ± 0.05[(e)]			
				4.4 ± 0.2	1.72 ± 0.03			
B	−116.0	0.93 (1)	14 ± 3	0.82 ± 0.08	3.02 ± 0.10	Si7	3.394 (6)	−116.3
C	−115.5	0.96 (1)	13 ± 3	0.82 ± 0.08	3.02 ± 0.10	Si5	3.418 (6)	−115.8
D	−114.4	1.06 (1)	13 ± 3					
E	−113.7	0.82 (1)	17 ± 3			Si2	3.851 (6)	−115.2
F	−113.3	1.16 (1)	15 ± 3	0.60 ± 0.08	3.35 ± 0.15	Si8	3.740 (6)	−114.4
G	−112.5	1.86 (2)	10 ± 3					
H	−111.6	1.78 (2)	25 ± 3	0.82 ± 0.10	3.02 ± 0.13	Si4	3.056 (6)	−113.7
I	−108.7	1.10 (1)	10 ± 3					
J	−107.5	4.45 (4)	32 ± 3	1.20 ± 0.10	2.66 ± 0.07	Si1	2.719 (6)	−110.4
K	−104.2	0.95 (1)	17 ± 3	0.80 ± 0.05	3.04 ± 0.06	Si6	3.259 (6)	−107.6

[a] Determined from ^{1}H→^{29}Si CP MAS spectrum at 15 kHz spin rate (Figure 2a). [b] Determined from ^{1}H→^{29}Si CP MAS spectrum at 1.9 kHz spin rate (Figure 3). [c] Determined by ^{19}F→^{29}Si CP MAS at 15 kHz (Figures 5 and 6), unless noted otherwise. [d] Calculated from the difference in the effective shielding anisotropy values of the *J*-coupled peaks (Figure 3). [e] Determined by ^{19}F→^{29}Si CP-REDOR at 15 kHz (Figure 4). [f] Based on the structure refinement of [F,DMABO]-STF presented in this paper. [g] Based on the linear correlation $\delta_{iso} = 247.6 - 116.7x$, where x = mean Si−Si distance.[47]

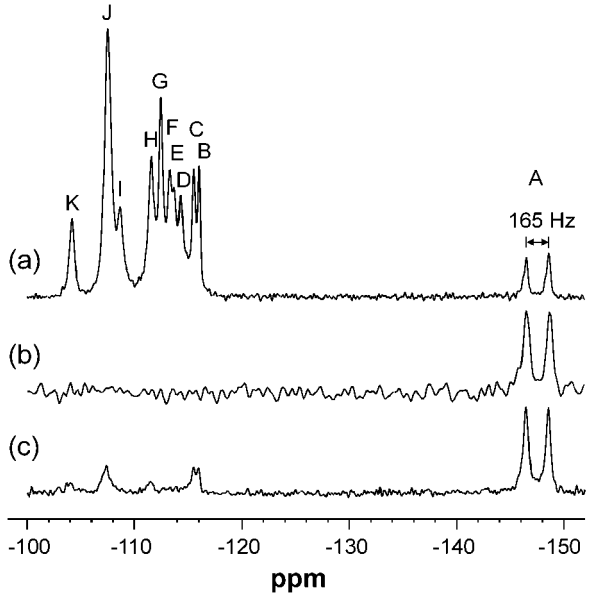

Figure 2. Fast spinning ^{29}Si NMR spectra of [F,DECDMP]-STF. (a) ^{1}H→^{29}Si CP MAS spectrum at 15 kHz spin rate and a contact time of 3 ms (6600 scans, 1.5 s recycle time). (b) ^{19}F→^{29}Si rotor-synchronized refocused INEPT experiment at 12 kHz spin rate (352 scans, 15 s recycle time). (c) ^{19}F→^{29}Si CP MAS spectrum at 15 kHz and a contact time of 0.4 ms (1000 scans, 15 s recycle time).

structure determined by XRD consists of one [$4^15^26^2$] cage with the bonded fluorine at 50% occupancy. This ^{29}Si MAS NMR spectrum suggests that the inversion center at (0.5, 0, 0.5) is not present at the local level and the asymmetric unit actually consists of a pair of fused [$4^15^26^2$] cages with the fluoride ion in only one of the cages with full occupancy as shown in Figure 1b. This confirms the proposal that the fluoride ions do not occupy both cages of this fused cage unit due to unfavorable electrostatic repulsions.[20] It is likely that these two samples differ in the degree of long-range ordering of the fluoride and SDA molecules for a number of possible reasons, including the nature of the SDA molecules. However, as this paper is concerned with the local structure of fluoride-containing STF zeolite, and in particular the local structure of the [$SiO_{4/2}F$]$^-$ unit, the differences in the long-range ordering in these samples is not of primary concern. It is, however, important to note that the local environment about one fluorine (as illustrated in Figure 1b) in these two samples is the same.

An important aspect of this spectrum is the two peaks of equal intensity at −146.5 and −148.6 ppm. These two peaks are actually a doublet centered at −147.6 ppm due to the ^{19}F/^{29}Si *J*-coupling of 165 Hz through the F−Si covalent bond. Clear evidence for the existence of the ^{19}F/^{29}Si *J*-coupling, and thus a covalent F−Si bond, is provided by the refocused INEPT experiment (Figure 2b), an NMR experiment in which polarization is transferred via the through-bond *J*-coupling. The close proximity of the fluoride ion to the silicon site associated with the doublet peak A is demonstrated by the ^{19}F→^{29}Si CP MAS experiment (Figure 2c), an NMR experiment in which polarization is transferred through-space via the dipolar interaction. The chemical shift, *J*-coupling, and strong ^{19}F/^{29}Si dipolar interaction clearly indicate that this doublet can be assigned to Si3. The less intense signals in the ^{19}F→^{29}Si CP MAS spectrum also indicate that the silicon sites associated with peaks B, C, H, J, and K are relatively close to the fluoride ion.

Five-Coordinate Silicon. At a much slower spin rate of 1.9 kHz, the *J*-coupled doublet centered at −147.6 ppm in the ^{1}H→^{29}Si CP MAS spectra changes considerably (Figure 3a). The peaks of the doublet no longer have equal intensities, an observation similar to that of Koller et al. for [F,DMABO]-ITE and [TPA,F]-MFI at low temperature.[15] The ^{19}F→^{29}Si CP MAS spectrum shows clearly that much of the intensity of the lower field resonance is distributed among a large number of spinning sidebands (Figure 3b). When all the spinning sidebands of the doublet are considered (Figure 3c), the total intensities are in fact equal as expected; the isotropic peaks have unequal intensities because the *effective* chemical shift anisotropy (CSA) tensors are quite different. The spinning sideband manifolds can be simulated well assuming an axially symmetric CSA tensor ($\eta = 0$) with effective shielding anisotropy (δ'_{aniso}) values of 9.8 ± 0.2 z and 2.0 ± 0.2 kHz for the resonances with δ_{iso} = −146.5 and −148.6 ppm, respectively (Figure 3d). The errors reported for these δ'_{aniso} values were estimated by comparing CSA patterns simulated with different δ'_{aniso} values to the experimental spectrum.

The large difference in the δ'_{aniso} values between the two peaks of the *J*-coupled doublet is due to the interplay of the CSA, dipolar coupling, and *J*-coupling tensors.[22−25] If the tensors are assumed to be collinear along the F−Si bond and the CSA tensor axially symmetric, the effective shielding anisotropy (δ'_{aniso}) depends on the actual shielding anisotropy (δ_{ansio}), the

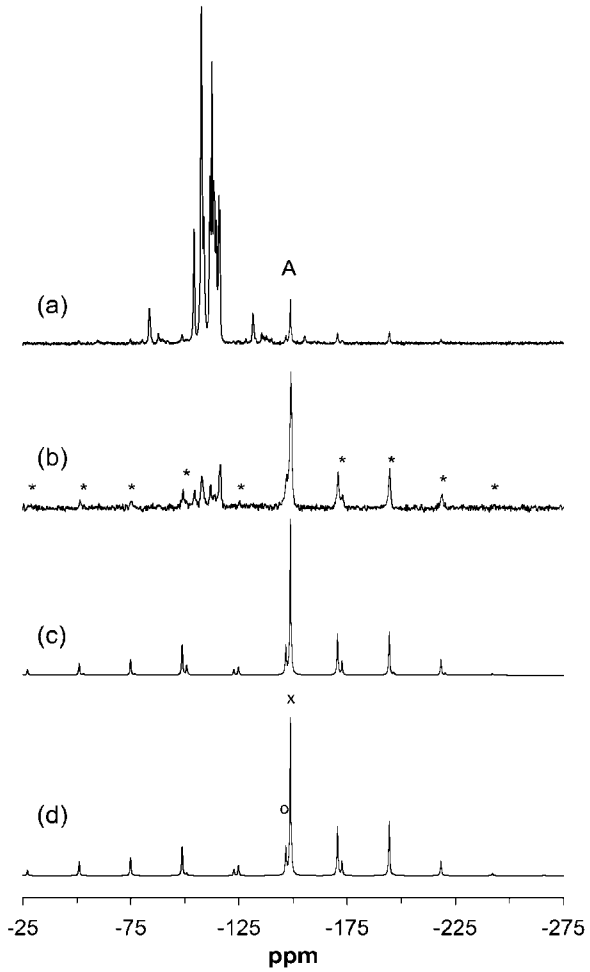

Figure 3. Slow spinning (1.9 kHz) ^{29}Si spectra of [F,DECDMP]-STF. (a) ^{1}H→^{29}Si CP MAS spectrum with 3 ms contact time (60 000 scans, 1.5 s recycle time). (b) ^{19}F→^{29}Si CP MAS spectra with 0.4 ms contact time (4580 scans, 15 s recycle time); spinning sidebands of the doublet peak A are indicated by asterisks. (c) Isotropic and spinning sidebands of peak A extracted from the ^{1}H→^{29}Si CP MAS spectrum; intensity is scaled by a factor of 4 relative to spectrum a. (d) Simulated effective CSA patterns of the doublets of peak A: (x) $\delta_{iso} = -148.6$ ppm, $\delta'_{aniso} = 2.0 \pm 0.2$ kHz, $\eta = 0$; (o) $\delta_{iso} = -147.5$ ppm, $\delta'_{aniso} = 9.8 \pm 0.2$ kHz, $\eta = 0$.

dipolar coupling (D), the anisotropy in J ($\Delta J = J_{\parallel} - J_{\perp}$), and the spin state of the nuclei ($m = \pm^1/_2$):[22]

$$\delta'_{aniso} = \delta_{aniso} - 2mD' = \delta_{aniso} \pm D' \qquad (1)$$

where the effective dipolar coupling is $D' = D - \Delta J/3$.

Using the δ'_{aniso} values determined from the ^{1}H→^{29}Si CP MAS spectrum, we get $\delta_{aniso} = 5.9 \pm 0.4$ kHz (74 ± 5 ppm) and $D' = 3.9 \pm 0.4$ kHz. If we assume that the anisotropy in J is small ($\Delta J \approx 0$), then the F−Si internuclear distance (r_{F-Si}) is calculated to be 1.79 ± 0.06 Å using

$$D = (\mu_0 \gamma_{Si} \gamma_F h)/(16\pi^3 r_{F-Si}{}^3). \qquad (2)$$

It is possible that the ^{19}F/^{29}Si dipolar coupling and F−Si distance obtained in this manner may have additional errors due to the assumptions that the CSA tensor is axially symmetric and collinear with the dipolar and J-coupling tensors. The large δ_{aniso} value compared to those of the other (tetrahedral) silicons (Table 2) is consistent with a large deviation from tetrahedral geometry.

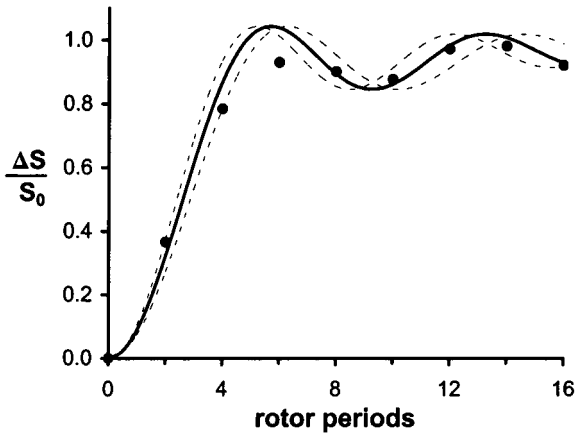

Figure 4. Experimental and simulated ^{19}F/^{29}Si CP-REDOR curves for Si3 (peak A) for [F,DECDMP]-STF at 15 kHz spin rate (304 scans per spectrum, 15 s recycle time). The data were fitted with a dipolar coupling of 4.4 ± 0.4 kHz, corresponding to a F−Si internuclear distance of 1.72 ± 0.05 Å. The solid line is the best fit and the dashed lines represent estimates of the error limits.

The ^{19}F/^{29}Si dipolar coupling and F−Si internuclear distance were also determined from a CP-REDOR experiment (Figure 4). Since the ^{19}F/^{29}Si dipolar coupling is strong, it was necessary to spin fast (15 kHz) to have sufficient time resolution in the REDOR experiment. The ^{19}F/^{29}Si dipolar coupling was determined to be 4.4 ± 0.4 kHz. Again, an effective dipolar coupling (D') is being measured,[46] so if we assume that the anisotropy in J is small ($\Delta J \approx 0$), the F−Si internuclear distance is calculated to be 1.72 ± 0.05 Å. The simulated REDOR curve (eq 7 in ref 16 or see the Supporting Information) does not fit the data exactly, but this is not entirely unexpected since, as the spin rate is fast, the duration of the ^{19}F 180° dephasing pulses is 15% of the rotor period, and the initial CP condition is set on a very narrow spinning sideband matching condition (isolated ^{19}F/^{29}Si spin pair). However, the period of the oscillation is fitted reasonably well, and we are confident that, given the results presented below, the calculated dipolar coupling is correct.

A third method of measuring the ^{19}F/^{29}Si dipolar coupling and F−Si internuclear distance is by a ^{19}F→^{29}Si variable contact time CP experiment.[16,28,37] In the case of isolated spin pairs, the CP curves will show an oscillation at a frequency that is proportional to the ^{19}F/^{29}Si dipolar coupling.[30] The ^{19}F→^{29}Si CP curve at the +1 spinning sideband matching condition for the Si3 resonance (peak A) is shown in Figure 5. The data were fitted using eq 1 in ref 16 (also provided in the Supporting Information). The dipolar coupling determined in this manner is 4.4 ± 0.2 kHz. Again, this dipolar coupling is an effective dipolar coupling (D'), and so if we assume $\Delta J \approx 0$, a F−Si internuclear distance of 1.72 ± 0.03 Å is obtained. Since five periods of the oscillation were observed and fit, the errors in the determined ^{19}F/^{29}Si dipolar coupling and F−Si internuclear distance are quite small. Although the two points at 0.6 and 0.7 ms are not fitted well by the simulated CP curves, it is clear that the period of oscillation is again fitted very well, and it is this that determines the dipolar coupling.

Four-Coordinate Silicons. Unfortunately, due to the relaxation behavior of this sample, it was not possible to perform a 2-D INADEQUATE experiment to assign the peaks to unique

(46) Holl, S. M.; Kowalewski, T.; Schaefer, J. *Solid State Nucl. Magn. Reson.* **1996**, *6*, 39.

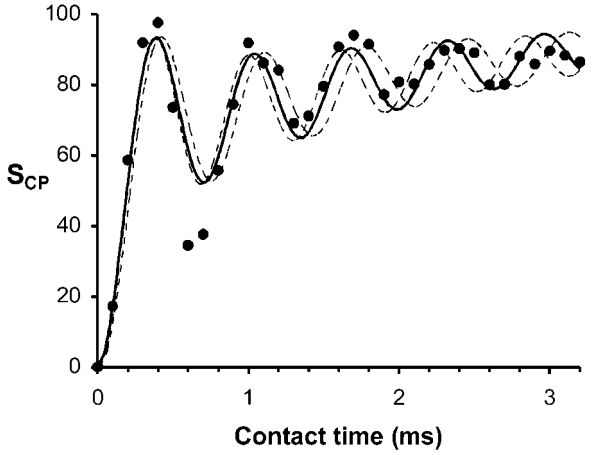

Figure 5. Experimental and simulated $^{19}F \rightarrow ^{29}Si$ CP curves for Si3 (peak A) of [F,DECDMP]-STF at the +1 spinning sideband matching condition with a 15 kHz spin rate (240 scans per spectrum, 15 s recycle time). The data were fitted with a dipolar coupling of 4.4 ± 0.2 kHz, corresponding to a F−Si internuclear distance of 1.72 ± 0.03 Å. The solid line is the best fit and the dashed lines represent estimates of the error limits.

silicon sites in the STF framework. It was difficult to obtain sufficient S/N since the ^{29}Si T_1 relaxation times were very long (~75 s) and although the ^1H T_1 relaxation time was short (1.2 s), the ^1H $T_{1\rho}$ relaxation time was also very short (3.4 ms), making the $^1H \rightarrow ^{29}Si$ CP experiment less efficient. In addition, since the ^{29}Si T_2 relaxation times were short (16 ms) there was a significant loss of signal during the echo in the INADEQUATE experiment. Nonetheless, it is possible to make a partial assignment of the peaks by considering the F−Si distances and δ_{iso} and δ_{aniso} values.

From the $^1H \rightarrow ^{29}Si$ CP MAS spectrum at 1.9 kHz spin rate (Figure 3a), the elements of the CSA tensor for each of the four-coordinate peaks can be obtained. Again, the tensors were assumed to be symmetric ($\eta = 0$). The fitted δ_{aniso} values for each peak are listed in Table 2. Since the ^{29}Si nuclei are usually in tetrahedral environments, the δ_{aniso} values are typically quite small. However, the existence of a F−Si covalent bond in the framework introduces significant distortion from tetrahedral geometry, which will manifest itself in increased δ_{aniso} values not only for the $[SiO_{4/2}F]^-$ units but also for the neighboring silicon atoms. Peaks E, H, J, and K have the largest δ_{aniso} values and therefore can be assigned to Si1, Si2, Si4, and Si6, which are the silicons in the coordination sphere of the five-coordinate Si3.

$^{19}F \rightarrow ^{29}Si$ CP curves were also determined for the four-coordinate peaks. The curves that show oscillatory behavior are shown in Figure 6. The measured dipolar couplings and F−Si internuclear distances are listed in Table 2. The complete fitting parameters are provided in the Supporting Information. Peak J gives an F−Si distance of 2.66 ± 0.07 Å so it is clear that Si1, which has a F−Si distance of 2.719 (6) Å in the XRD structure of [F,DMABO]-STF, is one of the four silicon sites that make up peak J. Because of the $1/r^3$ dependence of the dipolar coupling, this short F−Si distance will dominate the CP curve behavior. The measured δ_{aniso} value for peak J is also consistent with this assignment since Si1 is in the coordination sphere of Si3. Peaks B, C, H, and K all give F−Si distances of about 3 Å. The next four silicons closest to the fluoride ion with F−Si distances of about 3 Å are Si4, Si5, Si6, and Si7. Since peaks H and K have larger δ_{aniso} values, they can be assigned to Si4

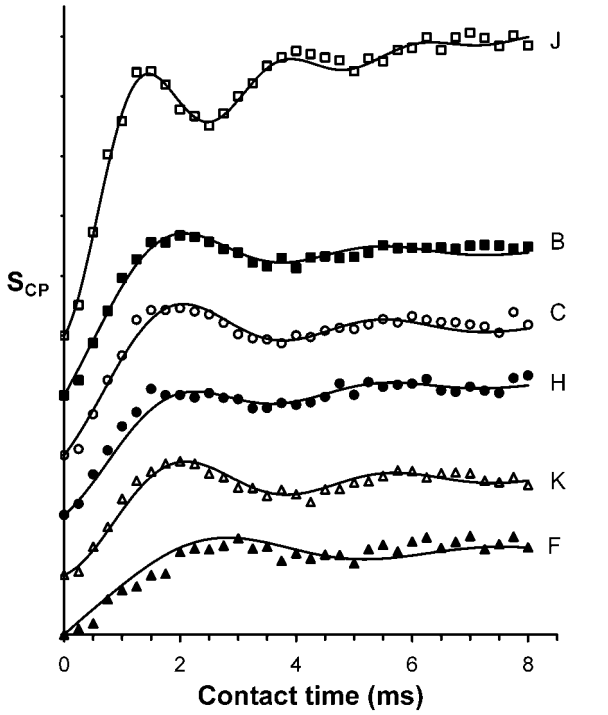

Figure 6. Experimental and fitted $^{19}F \rightarrow ^{29}Si$ CP curves for the four-coordinate peaks of [F,DECDMP]-STF (see Figure 2) at the +1 spinning sideband matching condition with a 15 kHz spin rate (504 scans per spectrum). The curves are offset from each other and at the same scale. The dipolar couplings obtained are listed in Table 2 and the complete fitting parameters are provided in the Supporting Information.

and Si6, while peaks B and C can be assigned to Si5 and Si7. Peak F gives a F−Si distance of 3.35 Å, which probably corresponds to the next nearest silicon, Si8. The larger δ_{aniso} value and longer F−Si distance of peak E (no oscillations observed) are consistent with an assignment of this peak to Si2.

The isotropic chemical shifts can also provide information about the peak assignments as they have been shown to correlate with average Si−Si distances (which incorporate both Si−O bond lengths and Si−O−Si bond angles) determined from XRD structures.[47] From the XRD crystal structure of [F,DMABO]-STF reported in this paper, isotropic chemical shifts were estimated from the average Si−Si distances by using this correlation. Although the predicted chemical shifts, presented in Table 2, do not agree absolutely with the measured δ_{iso} values (since the correlation is not based on fluoride-containing as-synthesized zeolites), the ordering is consistent. On the basis of these relative chemical shifts, it is possible to assign peak H to Si4 and peak K to Si6. Similarly, peak B is assigned to Si7 and peak C is assigned to Si5, although considering the errors involved, it is entirely possible that this last assignment could be reversed. The relative values of the predicted chemical shifts for the other peaks (E, F, J) are again consistent with the assignments made (Si2, Si8, Si1).

It is thus possible to assign half of the peaks in the $^1H \rightarrow ^{29}Si$ MAS spectrum to the silicon atoms which make up the $[4^15^26^2]$ cage in which the fluoride ion is located. Unfortunately, there is not enough information to reliably assign the remainder of the peaks related to the silicon atoms in the other $[4^15^26^2]$ cage where the fluoride ion is not present.

(47) Fyfe, C. A.; Feng, Y.; Grondey, H. *Microporous Mater.* **1993**, *1*, 393.

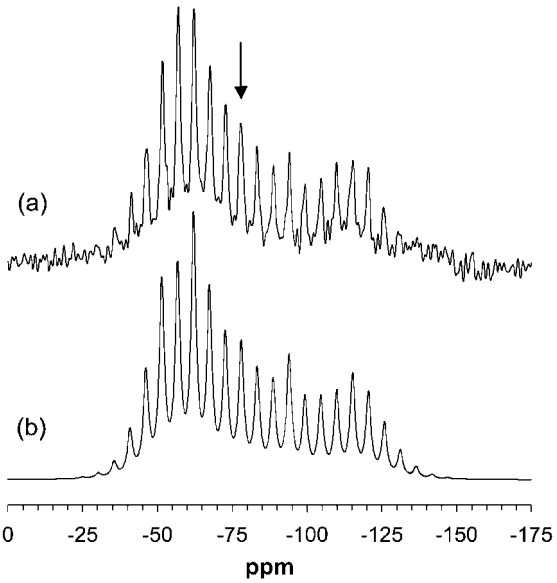

Figure 7. ^{19}F MAS NMR spectrum of [F,DECDMP]-STF. (a) Experimental spectrum at the 2.0 kHz spin rate. The recycle time was 100 s and 180 scans were collected. The isotropic peak is indicated by the arrow. (b) The simulated CSA pattern with $\delta_{iso} = -78.1$ ppm, $\delta_{aniso} = -54.2$ ppm, $\eta = 0.37$ ($\Omega = 91.5$ ppm).

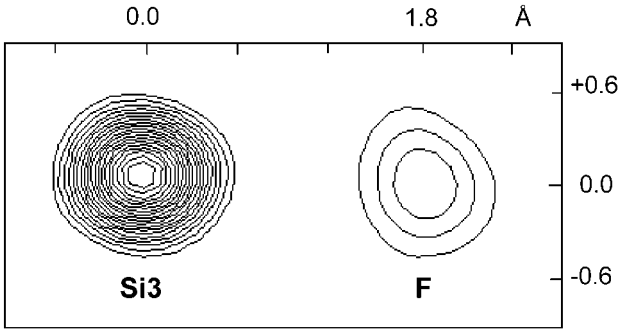

Figure 8. Contour plot of the difference ($F_o - F_c$) Fourier map computed in the O1−Si3−F1 plane. The Fourier map is calculated from the XRD data using a model containing all atoms except Si3 and F1 to calculate the phases. The map shows only two strong peaks representing the average Si3 position and the 50% occupied F1. The Si3 peak is almost spherical in shape and shows no evidence for splitting of the silicon electron density.

^{19}F MAS Spectrum. Koller and co-workers have established that the chemical shift of ^{19}F nuclei in rigid $[SiO_{4/2}F]^-$ units shows a characteristic behavior.[15] The isotropic chemical shift, $\delta_{iso} = (\delta_{11} + \delta_{22} + \delta_{33})/3$, is around −70 to −80 ppm and the span of the chemical shift tensor, $\Omega = \delta_{11} - \delta_{33}$, is about 80 to 87 ppm. Also, the anisotropy of the chemical shift tensor, $\delta_{aniso} = \delta_{33} - \delta_{iso}$, falls between −45 and −57 ppm. An analysis of the spinning sideband manifold in the ^{19}F MAS spectrum of [F,DECDMP]-STF (Figure 7) yields $\delta_{iso} = -78.1$ ppm, $\delta_{aniso} = -54.2$ ppm, and $\Omega = 91.5$ ppm, consistent with these previous observations.

Refinement of XRD Data Revisited. The F−Si internuclear distance measured in three separate solid-state NMR experiments on [F,DECDMP]-STF clearly indicates that it is significantly shorter than the 1.87 Å distance between the fluorine and an averaged silicon site as determined by the initial XRD refinement of [F,DMABO]-STF.[20] Also, the measured δ_{aniso} values for Si3 and its neighboring silicon atoms indicate significant distortions from tetrahedral geometry. Therefore, the XRD refinement of [F,DMABO]-STF was revisited in light of this new information.

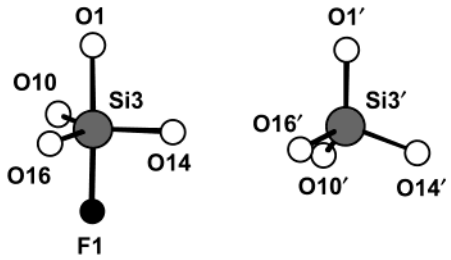

Figure 9. Coordination polyhedra around the disordered Si3/Si3′ pair. The coordination polyhedra are an almost perfect trigonal bipyramid around Si3 (left) and a tetrahedron around Si3′ (right). Distances and bond angles are listed in Table 3.

By careful examination of difference Fourier syntheses we have now located the $DMABO^+$ cation as disordered over two sites across the inversion center. The end of the SDA containing the nitrogen atom is relatively well defined with anisotropic displacement parameters (ADPs) of a reasonable magnitude. However, the carbon atoms progressively further away from the nitrogen atom have progressively larger ADPs, indicating less well defined positions and possibly some disorder.

In an attempt to detect the disorder between the tetrahedral $SiO_{4/2}$ and five-coordinate $[SiO_{4/2}F]^-$ pair, difference Fourier maps were calculated from the diffraction data, using the phases calculated from the structural model excluding Si3 and F. However, the resultant Fourier peaks (Figure 8) were almost spherical and showed no evidence for a resolution of the average Si3 position into two distinct positions, although the electron density at Si3 is very slightly elongated along the F−Si bond. This indicates that the fundamental resolution of the XRD experiment is not quite sufficient to fully resolve this disorder in the structure and demonstrates the importance of the solid-state NMR measurements.

However, refinement of a disordered model with two resolved silicon sites (Si3 and Si3′) and the four oxygen atoms in their coordination spheres and isotropic displacement parameters for these "split" atoms was stable and yielded a F−Si distance of 1.744 (7) Å in very good agreement with that determined from the NMR experiments on [F,DECDMP]-STF. Furthermore, this refinement resulted in a reasonable trigonal bipyramidal $[SiO_{4/2}F]^-$ unit and a tetrahedral $SiO_{4/2}$ unit, with slightly elongated equatorial Si−O distances and a significantly longer axial Si−O distance when compared to distances in SiO_4 tetrahedra (Figure 9 and Table 3). The $O_{ax}-Si-O_{eq}$ angles are very close to 90° but the $O_{eq}-Si-O_{eq}$ angles have a slightly larger range (from 112° to 126°). It should be remembered that the coordinations of the $[SiO_{4/2}F]^-$ units are constrained by the rigidity/flexibility of the zeolite framework itself. The DFT calculations performed by Attfield and co-workers[27] on fluoride-containing SOD and FER frameworks showed a similar coordination variation between frameworks, and the small deviations from perfect trigonal-bipyramidal coordination may well be real.

When the disordered model was refined using ADPs for all atoms, the "split" silicon sites merged back to the average position and their ADPs became physically unreasonable. This

(48) Fyfe, C. A.; Shajani, Z.; Lewis, A. R.; Groat, L. To be submitted for publication.

Table 3. Bond Lengths (Å) and Angles (deg) around Five-Coordinate Si3 and Tetrahedral Si3′

Si3 (5-coordinate)		Si3′ (tetrahedral)	
Si3−F1	1.744 (7)		
Si3−O1	1.76 (1)	Si3′−O1′	1.581 (9)
Si3−O10	1.666 (9)	Si3′−O10′	1.587 (9)
Si3−O14	1.633 (8)	Si3′−O14′	1.609 (8)
Si3−O16	1.650 (9)	Si3′−O16′	1.598 (8)
O10−Si3−O14	112.6 (4)	O10′−Si3′−O14′	110.2 (5)
O10−Si3−O16	121.0 (5)	O10′−Si3′−O16′	112.7 (4)
O14−Si3−O16	126.2 (5)	O14′−Si3′−O16′	104.0 (4)
O1−Si3−O10	90.1 (5)	O1′−Si3′−O10′	109.8 (5)
O1−Si3−O14	92.9 (5)	O1′−Si3′−O14′	110.8 (5)
O1−Si3−O16	90.7 (5)	O1′−Si3′−O16′	109.2 (5)
F1−Si3−O1	178.1 (4)		
F1−Si3−O10	88.7 (4)		
F1−Si3−O14	88.4 (4)		
F1−Si3−O16	89.1 (4)		

is not unexpected as the resolution of the XRD data (d_{min} = 0.7 Å) is not sufficient to fully resolve this disorder since the separation between the "split" silicon sites with isotropic displacement parameters is only 0.25 Å. However, the excellent agreement between the results of the isotropic refinement on [F,DMABO]-STF, the NMR results on [F,DECDMP]-STF, and the results of DFT simulations carried out by Attfield and coworkers[27] on SOD and FER frameworks indicates that the local structure of the $[SiO_{4/2}F]^-$ unit is indeed trigonal bipyramidal, with an F−Si bond length of approximately 1.72−1.79 Å. It might be supposed that other framework structures would show similar local structures around the five-coordinate silicon atoms. Indeed, XRD refinements of low-temperature data for a [F,-BQol]-IFR microcrystal (similar framework structure to STF) and a twinned [F,TPA]-MFI[48] crystal result in very similar disordered models, with almost perfectly trigonal-bipyramidal $[SiO_{4/2}F]^-$ units having F−Si distances (1.78 (1) and 1.77 (1) Å respectively) within the experimental error found for the STF framework structures.

The relationship between the structures of [F,DMABO]-STF and [F,DECDMP]-STF is of interest because it may provide further information on the long-range structure-directing effects of fluoride ions and SDA molecules, although it was not necessary for the determination of the local structure of the $[SiO_{4/2}F]^-$ unit. The broader ^{29}Si resonances of the [F,DMABO]-STF sample might reflect the disorder detected by the diffraction study, but could also be caused by small numbers of defects to which diffraction is not sensitive. In the case of [F,DECDMP]-STF, the narrow resonances could indicate perfect ordering over whole crystallites, but could also be due to ordering over more limited volumes, or even no ordering depending on the sensitivity of the ^{29}Si spectrum to the ordering, which at present has not been established. Further work to address these points is in progress.

Conclusions

The combination of magic angle spinning NMR and microcrystal XRD experiments makes it possible to fully elucidate the local structure of the five-coordinate silicon in as-made zeolites with the STF framework structure. Three different NMR methods on [F,DECDMP]-STF, slow spinning MAS, variable contact time CP, and REDOR, yielded F−Si distances that were not significantly different from each other but were markedly shorter than that found from previous "average" single-crystal XRD experiments. A subsequent revisiting of the XRD refinement of [F,DMABO]-STF, this time including terms to take account of the disorder present, resulted in a F−Si distance in almost perfect agreement with those found from the NMR experiments. However, the XRD experiment is not of high enough resolution to fully determine the disordered model with anisotropic displacement parameters. This is a splendid example where, without the results from the NMR experiments, there would always be doubt about the accuracy of the XRD study. The use of the two techniques together is a powerful combination that has allowed us to determine the coordination of the $[SiO_{4/2}F]^-$ unit as being an almost perfect trigonal bipyramid.

Acknowledgment. The authors would like to thank the Natural Sciences and Engineering Council of Canada for Operating and Equipment grants (C.A.F.) and for the award of a Postgraduate Fellowship (D.H.B.), the Engineering and Physical Sciences Research Council (UK) for grants (L.A.V. and R.E.M.), and the Royal Society for the provision of a University Research Fellowship (R.E.M.). We would also like to thank one of the referees whose suggestions prompted us to consider the relationship between the two STF samples with greater care.

Supporting Information Available: Details of the crystal structure determination (CIF) and fitting of the CP curves (PDF). This material is available free of charge via the Internet at http://pubs.acs.org.

JA012558S